

Kinetics and Mechanism of the Oxidation of Hydroquinones by a *trans*-Dioxoruthenium(VI) Complex

William W. Y. Lam, Mendy F. W. Lee, and Tai-Chu Lau*

Department of Biology and Chemistry, City University of Hong Kong, Tat Chee Avenue, Kowloon Tong, Hong Kong, China

Received August 13, 2005

The kinetics of the oxidation of hydroquinone (H₂Q) and its derivatives (H₂Q-X) by *trans*-[Ru^{VI}(tmc)(O)₂]²⁺ (tmc = 1,4,8,11-tetramethyl-1,4,8,11-tetraazacyclotetradecane) have been studied in aqueous acidic solutions and in acetonitrile. In H₂O, the oxidation of H₂Q has the following stoichiometry: *trans*-[Ru^{VI}(tmc)(O)₂]²⁺ + H₂Q → *trans*-[Ru^{IV}(tmc)(O)(OH)₂]²⁺ + Q. The reaction is first order in both Ru^{VI} and H₂Q, and parallel pathways involving the oxidation of H₂Q and HQ⁻ are involved. The kinetic isotope effects are $k(\text{H}_2\text{O})/k(\text{D}_2\text{O}) = 4.9$ and 1.2 at pH = 1.79 and 4.60, respectively. In CH₃CN, the reaction occurs in two steps, the reduction of *trans*-[Ru^{VI}(tmc)(O)₂]²⁺ by 1 equiv of H₂Q to *trans*-[Ru^{IV}(tmc)(O)(CH₃CN)]²⁺, followed by further reduction by another 1 equiv of H₂Q to *trans*-[Ru^{II}(tmc)(CH₃CN)₂]²⁺. Linear correlations between log(rate constant) at 298.0 K and the O–H bond dissociation energy of H₂Q–X were obtained for reactions in both H₂O and CH₃CN, consistent with a H-atom transfer (HAT) mechanism. Plots of log(rate constant) against log(equilibrium constant) were also linear for these HAT reactions.

Introduction

Hydroquinones are well-known two-electron reductants that play important roles in biological electron transport processes.¹ The oxidation of these compounds by transition-metal complexes has been extensively studied.^{2–10} These oxidants include [Ni^{III}(cyclam)]³⁺,² [Ni^{IV}(oxime)]²⁺,³ [Mn^{III}(EDTA)]⁻,⁴ [Rh₂(O₂CCH₃)₄(OH)₂]⁺,⁵ iron(II) porphyrins,⁶

[Cu^{II}(dmp)₂]²⁺,⁷ [Ru^{III}(CN)₆]³⁻,⁸ VO²⁺,⁹ and Cu²⁺(aq).¹⁰ These reactions usually involve a rate-determining one-electron oxidation of the hydroquinone to a semiquinone radical followed by a second one-electron oxidation to the quinone, by either an inner- or outer-sphere mechanism. On the other hand, the oxidation of hydroquinone by [Ru^{IV}(bpy)(py)(O)]²⁺ and [Ru^{III}(bpy)(py)(OH)]²⁺ proceeds through a proton-coupled electron-transfer (PCET) mechanism.¹¹

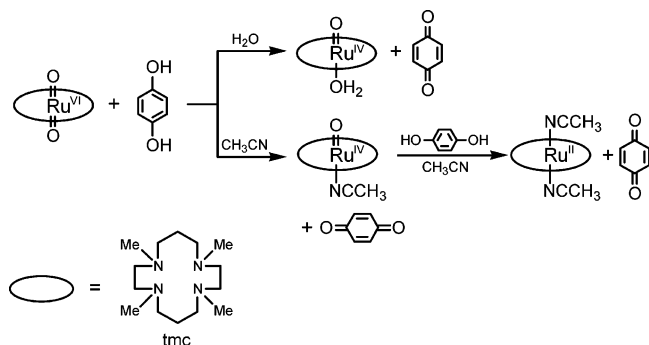
We report here the results of a kinetics and mechanistic study of the oxidation of a series of hydroquinones in both aqueous solutions and acetonitrile by a cationic *trans*-dioxoruthenium(VI) complex, *trans*-[Ru^{VI}(tmc)(O)₂]²⁺ (tmc = 1,4,8,11-tetramethyl-1,4,8,11-tetraazacyclotetradecane; Scheme 1).¹² These reactions are shown in Scheme 1. The relationship between the reactivity and O–H bond strengths of the hydroquinones was examined. *trans*-[Ru^{VI}(tmc)(O)₂]²⁺ contains a macrocyclic tertiary amine ligand (tmc) that is resistant to oxidative degradation and ligand exchange. It is a mild oxidant with well-defined redox potentials. The lower oxidation states of this complex (V–II) are also well-

* To whom correspondence should be addressed. E-mail: bhtclau@cityu.edu.hk.

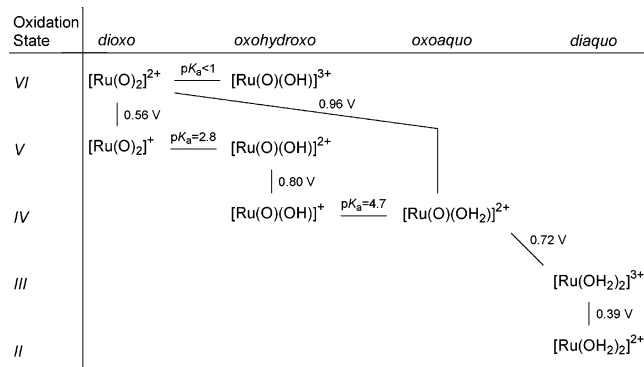
- (1) (a) Chambers, J. Q. In *The Chemistry of Quinonoid Compounds*; Patai, S., Rappaport, Z., Eds.; John Wiley and Sons: New York, 1988; Vol. II, p 719. (b) Lemberg, R. Barret, J. *Cytochromes*; Academic Press: London, 1973. (c) Rich, P. R. *Faraday Discuss. Chem. Soc.* **1982**, *74*, 349.
- (2) Brodovitch, J. C.; McAuley, A.; Oswald, T. *Inorg. Chem.* **1982**, *21*, 3442–3447.
- (3) Macartney, D. H.; McAuley, A. *J. Chem. Soc., Dalton Trans.* **1984**, 103–107.
- (4) Giraudi, G.; Mentasti, E. *Transition Met. Chem.* **1981**, *6*, 230–234.
- (5) Herbert, J. W.; Macartney, D. H. *J. Chem. Soc., Dalton Trans.* **1986**, 1931–1935.
- (6) Castro, C. E.; Hathaway, G. M.; Havlin, R. *J. Am. Chem. Soc.* **1977**, *99*, 8032–8039.
- (7) Clemmer, J. D.; Hogaboom, G. K.; Holwerda, R. A. *Inorg. Chem.* **1979**, *18*, 2567–2572.
- (8) Hoddenbagh, J. M. A.; Macartney, D. H. *J. Chem. Soc., Dalton Trans.* **1990**, 615–620.
- (9) Kustin, K.; Liu, S.-T.; Nicolini, C.; Toppen, D. L. *J. Am. Chem. Soc.* **1974**, *96*, 7410–7415.
- (10) Kamau, P.; Jordan, R. B. *Inorg. Chem.* **2002**, *41*, 3076–3083.

- (11) Binstead, R. A.; McGuire, M. E.; Dovletoglou, A.; Seok, W. K.; Roecker, L. E.; Meyer, T. J. *J. Am. Chem. Soc.* **1992**, *114*, 173–186.
- (12) (a) Che, C. M.; Wong, K. Y.; Poon, C. K. *Inorg. Chem.* **1985**, *24*, 1797–1800. (b) Che, C. M.; Lai, T. F.; Wong, K. Y. *Inorg. Chem.* **1987**, *26*, 2289–2299.

Scheme 1



Scheme 2



characterized. The oxidation of alcohols,¹³ alkenes,¹⁴ $[\text{Fe}(\text{H}_2\text{O})_6]^{2+}$,¹⁵ iodide,¹⁶ sulfite,¹⁷ and a number of outer-sphere ruthenium(II) reductants¹⁸ by $\text{trans-}[\text{Ru}^{\text{VI}}(\text{tmc})(\text{O})_2]^{2+}$ has been reported. Thermodynamic data (E° vs NHE and pK_a values, 298 K) for the $\text{trans-}[\text{Ru}^{\text{VI}}(\text{tmc})(\text{O})_2]^{2+}$ system are summarized in Scheme 2.^{12a,18}

Experimental Section

Materials. $\text{trans-}[\text{Ru}^{\text{VI}}(\text{tmc})(\text{O})_2](\text{PF}_6)_2$ and $\text{trans-}[\text{Ru}^{\text{IV}}(\text{tmc})(\text{O})(\text{CH}_3\text{CN})](\text{PF}_6)_2$ were prepared according to the literature.¹² Hydroquinone (H_2Q) was obtained from Reidel-deHaen and was recrystallized from ethanol.¹⁹ 2,5-Di-*tert*-butylhydroquinone (Aldrich) was recrystallized from glacial acetic acid.¹⁹ All other hydroquinones ($\text{H}_2\text{Q-X}$) were of reagent grade and were used as received. Water for kinetic experiments was distilled twice from alkaline permanganate. The ionic strength was maintained with sodium trifluoroacetate. Acetonitrile (analytical reagent grade) was refluxed overnight with KMnO_4 and then distilled. It was further distilled over CaH_2 under argon. $\text{H}_2\text{Q-}d_6$ (98 atom % D, Cambridge Isotope) and D_2O (99.8 atom % D, AcrôS) were used as received. The pD values for all D_2O solutions were determined either by

titration with standard NaOH solutions or by using a pH meter with the relationship $pD = \text{pH}_{\text{meas}} + 0.4$.

Kinetics. The kinetics of the reaction were studied by using either a Hewlett-Packard 8452A diode array spectrophotometer, an Applied Photophysics SX-17MV, or a Hi-Tech SF-61 stopped-flow spectrophotometer. The concentrations of $\text{H}_2\text{Q-X}$ were at least in 10-fold excess of that of Ru^{VI} . The reaction progress was monitored by observing absorbance changes at 246 nm. Pseudo-first-order rate constants, k_{obs} , were obtained by nonlinear least-squares fits of A_t vs t according to the equation $A_t = A_\infty + (A_0 - A_\infty) \exp(-k_{\text{obs}}t)$, where A_0 and A_∞ are the initial and final absorbances, respectively. For reactions that occur in two steps, the sequential pseudo-first-order rate constants were calculated by fitting the kinetic trace to a biexponential function.²⁰

Product Analysis. For Reactions in Aqueous Solutions. The ruthenium product for the reduction of Ru^{VI} by H_2Q in aqueous solutions was determined by the following procedure. A known amount of $\text{trans-}[\text{Ru}^{\text{VI}}(\text{tmc})(\text{O})_2]^{2+}$ (1.0×10^{-4} M) was allowed to react with an excess amount of H_2Q (4.0×10^{-3} M) at 298.0 K, $\text{pH} = 1.49$ and $I = 0.1$ M. The resulting solution was loaded onto a Sephadex-SP C-25 cation-exchange column. By elution with 0.2 M $\text{CF}_3\text{CO}_2\text{H}$ and then examination of the UV-vis spectrum of the solution, $\text{trans-}[\text{Ru}^{\text{IV}}(\text{tmc})(\text{O})(\text{OH}_2)]^{2+}$ ($\lambda_{\text{max}} = 290$ nm, $\epsilon = 1600$ $\text{M}^{-1} \text{cm}^{-1}$)¹² was found to be produced quantitatively.

The organic products were determined by UV-vis spectrophotometry and gas chromatography (GC). In a typical UV-vis spectrophotometric determination, $\text{trans-}[\text{Ru}^{\text{VI}}(\text{tmc})(\text{O})_2]^{2+}$ (2.5×10^{-5} M) was allowed to react with H_2Q (1×10^{-4} M) at $\text{pH} = 4.67$. After the reaction was completed (ca. 5 min), the solution was loaded onto a Sephadex-SP C-25 cation-exchange column and eluted with water. The UV-vis spectrum of the eluted solution showed the presence of 2.4×10^{-5} M *p*-benzoquinone (Q; $\lambda_{\text{max}} = 246$ nm, $\epsilon = 2.0 \times 10^4$ $\text{M}^{-1} \text{cm}^{-1}$),²¹ corresponding to a yield of 94%.

In GC determination of organic products, a Hewlett-Packard 5890 gas chromatograph equipped with a DB-5MS capillary column and a Hewlett-Packard 5890 gas chromatograph interfaced with a HP5970 mass selective detector were used. The analysis of the products resulting from the oxidation of H_2Q was typically carried out as follows. Ru^{VI} (4.8×10^{-3} mmol) was added to H_2Q (4.8×10^{-2} mmol) in 1 mL of H_2O at room temperature in the dark with vigorous stirring. After 10 min, analysis by GC-mass spectrometry (MS) indicated the presence of Q. Qualitative analysis by GC with a flame ionization detector indicated that 4.4×10^{-3} mmol of Q was produced, corresponding to a yield of 92%. This is in good agreement with the yield obtained by the UV-vis method.

For Reactions in CH_3CN . Typically, a known amount of $\text{trans-}[\text{Ru}^{\text{VI}}(\text{tmc})(\text{O})_2]^{2+}$ (2.5×10^{-5} M) was allowed to react with H_2Q (1×10^{-4} M) in CH_3CN . After 10 min, the amount of Q produced was determined spectrophotometrically at 246 nm, taking into account the absorbance due to the $\text{trans-}[\text{Ru}^{\text{II}}(\text{tmc})(\text{CH}_3\text{CN})_2]^{2+}$ product at this wavelength.²² 5.2×10^{-5} M Q was found, and the ratio of Q formed with Ru^{VI} used is 2.1 ± 0.1 . $\text{trans-}[\text{Ru}^{\text{II}}(\text{tmc})(\text{CH}_3\text{CN})_2]^{2+}$ was found to be produced quantitatively by evaporating the solution after reaction to dryness, extracting the organics with diethyl ether, and then examining the UV-vis spectrum of the residue in CH_3CN .

- (13) Che, C. M.; Tang, W. T.; Lee, W. O.; Wong, K. Y.; Lau, T. C. *J. Chem. Soc., Dalton Trans.* **1992**, 1551–1556.
 (14) Che, C. M.; Li, C. K.; Tang, W. T.; Yu, W. Y. *J. Chem. Soc., Dalton Trans.* **1992**, 3153–3158.
 (15) Lau, T. C.; Lau, K. W. C.; Lo, C. K. *Inorg. Chim. Acta* **1993**, 209, 89–92.
 (16) Lau, T. C.; Lau, K. W. C.; Lau, K. *J. Chem. Soc., Dalton Trans.* **1994**, 3091–3093.
 (17) Lau, T. C.; Chow, K. H.; Lau, K. W. C.; Tsang, W. Y. K. *J. Chem. Soc., Dalton Trans.* **1997**, 313–315.
 (18) Che, C. M.; Lau, K.; Lau, T. C.; Poon, C. K. *J. Am. Chem. Soc.* **1990**, 112, 5176–5181.
 (19) Armarego, W. L. F.; Perrin, D. D. *Purification of Laboratory Chemicals*, 4th ed.; Reed Educational and Professional Publishing Ltd.: Oxford, U.K., 1996.

- (20) Espenson, J. H. *Chemical Kinetics and Reaction Mechanisms*, 2nd ed.; McGraw-Hill: New York, 1995; pp 72–76.
 (21) Kettle, A. J.; Winterbourn, C. C. *J. Biol. Chem.* **1992**, 267, 8319–8324.
 (22) Che, C. M.; Wong, K. Y.; Poon, C. K. *Inorg. Chem.* **1986**, 25, 1809–1813.

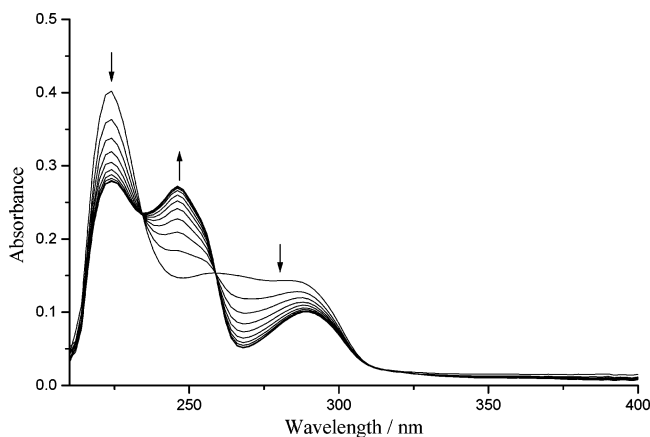
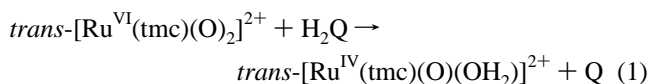


Figure 1. Spectrophotometric changes at 2000-s intervals during the oxidation H_2Q (5×10^{-5} M) by $\text{trans-}[\text{Ru}^{\text{VI}}(\text{tmc})(\text{O})_2]^{2+}$ (2.5×10^{-5} M) at 298.0 K, pH = 2.06 and $I = 0.1$ M.

Results

Reactions in H_2O . Spectrophotometric Changes and Products. Figure 1 shows the spectrophotometric changes when a solution of $\text{trans-}[\text{Ru}^{\text{VI}}(\text{tmc})(\text{O})_2]^{2+}$ (2.5×10^{-5} M) was mixed with a solution of H_2Q (5×10^{-5} M) at 298.0 K, pH = 2.06 and $I = 0.1$ M. Well-defined isosbestic points at 234, 258, and 312 nm were maintained throughout the course of the reaction. The growth of a peak at around 246 nm indicated the formation of Q,¹¹ which was also detected by GC–MS. Examination of the final spectrum after removal of the organics by column chromatography indicated quantitative formation of $\text{trans-}[\text{Ru}^{\text{IV}}(\text{tmc})(\text{O})(\text{OH}_2)]^{2+}$ (see the Experimental Section). Further reduction of $\text{trans-}[\text{Ru}^{\text{IV}}(\text{tmc})(\text{O})(\text{OH}_2)]^{2+}$ was not observed for at least 3 h.

The oxidation of H_2Q results in the formation of over 90% Q as determined by UV–vis and GC (see the Experimental Section). The yields are based on $\text{trans-}[\text{Ru}^{\text{VI}}(\text{tmc})(\text{O})_2]^{2+}$ acting as a two-electron oxidant. No other organic products were detected. The stoichiometry of the reaction can be represented by eq 1.



Kinetics. The kinetics of the reaction shown in eq 1 were followed at 246 nm, the absorption maximum of Q. In the presence of at least 10-fold excess of H_2Q , clean pseudo-first-order kinetics were observed for over 3 half-lives. No induction periods were observed. The pseudo-first-order rate constant, k_{obs} , is independent of the concentration of the Ru^{VI} complex (2.5×10^{-5} – 1×10^{-4} M) but depends linearly on the concentration of H_2Q . The experimentally determined rate law is as shown in eq 2.

$$-\frac{d[\text{Ru}^{\text{VI}}]}{dt} = k_{\text{H}_2\text{O}}[\text{H}_2\text{Q}][\text{Ru}^{\text{VI}}] = k_{\text{obs}}[\text{Ru}^{\text{VI}}] \quad (2)$$

Effects of Acidity. The effects of acidity on the rate constant were studied over the range pH = 1–5 at 298.0 K

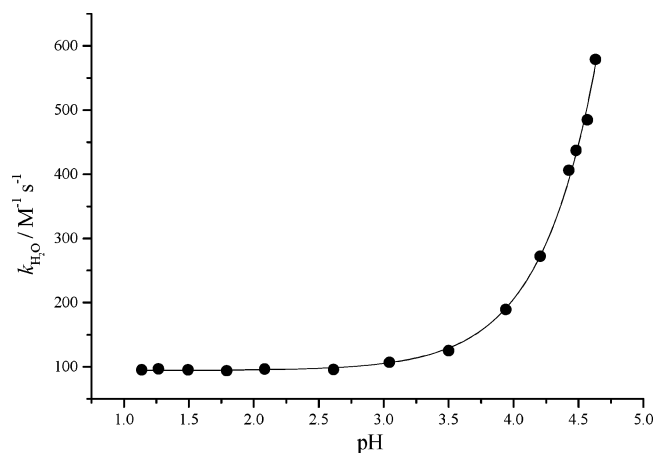


Figure 2. Plot of $k_{\text{H}_2\text{O}}$ vs pH for the oxidation of H_2Q by $\text{trans-}[\text{Ru}^{\text{VI}}(\text{tmc})(\text{O})_2]^{2+}$ at 298.0 K and $I = 0.1$ M.

and $I = 0.1$ M. At higher pH, Ru^{VI} is not very stable. $k_{\text{H}_2\text{O}}$ is nearly constant below pH = 3 but increases rapidly above pH = 3.5 (Figure 2). The data were fitted to eq 3.

$$k_{\text{H}_2\text{O}} = \frac{k_a[\text{H}^+] + k_b K_a}{[\text{H}^+] + K_a} \quad (3)$$

K_a is the acid dissociation constant of H_2Q and is taken as 1.41×10^{-10} M at 298.0 K.²³ k_a and k_b are the rate constants for the oxidation of H_2Q and HQ^- , respectively. At 298.0 K and $I = 0.1$ M, k_a and k_b are $(9.41 \pm 0.28) \times 10^1$ and $(7.91 \pm 0.10) \times 10^7 \text{ M}^{-1} \text{ s}^{-1}$, respectively.

Activation Parameters. The effects of temperature on the oxidation of H_2Q by Ru^{VI} were studied from 288.0 to 318.0 K at pH = 1.16 and $I = 0.1$ M. At pH = 1.16, the pathway for the oxidation of HQ^- is negligible. Activation parameters were obtained from the plot of $\ln(k_{\text{H}_2\text{O}}/T)$ vs $1/T$ according to the Eyring equation. ΔH^\ddagger and ΔS^\ddagger are found to be 12.3 ± 0.1 kcal mol⁻¹ and $-(8 \pm 1)$ cal mol⁻¹ K⁻¹, respectively.

Kinetic Isotope Effects. The kinetics were carried out in D_2O at $T = 298.0$ K and $I = 0.1$ M. At pH = 1.79, the solvent kinetic isotope effect, $k(\text{H}_2\text{O})/k(\text{D}_2\text{O}) = 4.9 \pm 0.3$. On the other hand, at pH = 4.60, $k(\text{H}_2\text{O})/k(\text{D}_2\text{O}) = 1.20 \pm 0.2$. However, at both pHs, the oxidation of $\text{H}_2\text{Q-}d_6$ in H_2O shows no kinetic isotope effects, $k[\text{C}_6\text{H}_4(\text{OH})_2]/k[\text{C}_6\text{D}_4(\text{OD})_2] = 1.0$.

Oxidation of Substituted H_2Q . The kinetics of the oxidation of various substituted H_2Q ($\text{H}_2\text{Q-X}$) by Ru^{VI} have been investigated in aqueous solutions at pH = 1.78 at 298.0 K; at this pH, the pathway involving HQ-X^- is negligible. The spectrophotometric changes are the kinetic behavior for the oxidation of $\text{H}_2\text{Q-X}$ substrates are similar to that of the parent H_2Q . Representative data are collected in Table 1.

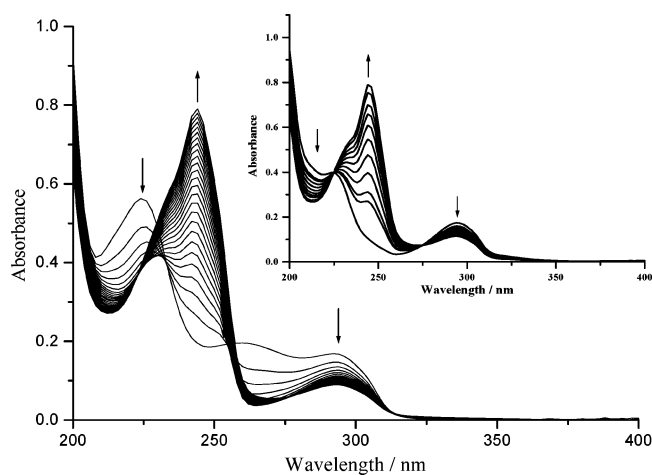
Reactions in CH_3CN . In contrast to the reaction in water, the spectrophotometric changes for the oxidation of H_2Q by $\text{trans-}[\text{Ru}^{\text{VI}}(\text{tmc})(\text{O})_2]^{2+}$ in CH_3CN indicate biphasic behavior (Figure 3). The first step shows isosbestic points at 234 and 254 nm, while the second step shows isosbestic points at

(23) McAuley, A.; MacDonald, C. J.; Spencer, L.; West, P. R. *J. Chem. Soc., Dalton Trans.* **1988**, 2279–2286.

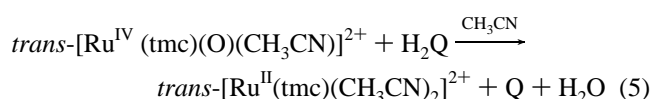
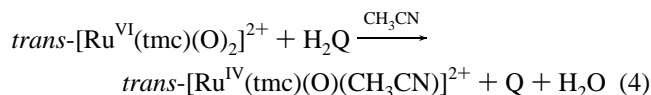
Table 1. Summary of the Second-Order Rate Constants for the Oxidation of H₂Q-X by *trans*-[Ru^{VI}(tmc)(O)₂]²⁺ in Both Aqueous Solutions and Acetonitrile at 298.0 K

substrate	$k_{\text{H}_2\text{O}}/\text{M}^{-1} \text{s}^{-1}{}^a$	$k_{\text{ACN}}/\text{M}^{-1} \text{s}^{-1}{}^b$	$k'_{\text{ACN}}/\text{M}^{-1} \text{s}^{-1}{}^b$
2,5-di-'Bu	$(5.62 \pm 0.05) \times 10^2$	$(2.51 \pm 0.17) \times 10^2$	$(1.00 \pm 0.09) \times 10^1$
'Bu	$(7.21 \pm 0.15) \times 10^2$	$(3.50 \pm 0.52) \times 10^2$	$(1.18 \pm 0.05) \times 10^1$
2,3-di-Me	$(6.60 \pm 0.02) \times 10^2$	$(2.90 \pm 0.14) \times 10^2$	$(1.13 \pm 0.04) \times 10^1$
Me	$(6.05 \pm 0.04) \times 10^2$	$(2.24 \pm 0.06) \times 10^2$	8.44 ± 0.13
OMe	$(3.18 \pm 0.03) \times 10^2$	$(1.73 \pm 0.08) \times 10^2$	5.40 ± 0.14
H	$(9.37 \pm 0.12) \times 10^1$	$(8.53 \pm 0.32) \times 10^1$	2.21 ± 0.04
Cl	$(5.19 \pm 0.06) \times 10^1$	$(3.44 \pm 0.16) \times 10^1$	1.49 ± 0.06
2,3-di-CN	1.27 ± 0.07^c	1.00 ± 0.04	$(4.70 \pm 0.07) \times 10^{-2}$

^a Experiments were carried out in aqueous solution at pH = 1.8 and $I = 0.1$ M unless specified. ^b Experiments were carried out in CH₃CN. k_{ACN} and k'_{ACN} are the rate constants for the first and second steps, respectively. ^c Experiment was carried out at pH = 1.0.

**Figure 3.** Spectrophotometric changes at 864-s intervals for the oxidation of H₂Q (5×10^{-5} M) by *trans*-[Ru^{VI}(tmc)(O)₂]²⁺ (2.5×10^{-5} M) in CH₃CN at 298.0 K. The inset shows the oxidation of H₂Q (5×10^{-5} M) by *trans*-[Ru^{IV}(tmc)(O)(CH₃CN)]²⁺ (2.5×10^{-5} M) in CH₃CN at 298.0 K at 200-s intervals.

224 and 280 nm. The final spectrum (after removal of organics) shows the quantitative formation of *trans*-[Ru^{II}(tmc)(CH₃CN)₂]²⁺.²² The spectrophotometric changes for the second step are identical with those for the reaction of H₂Q with *trans*-[Ru^{IV}(tmc)(O)(CH₃CN)]²⁺. Also, 2 mol of Q is formed from 1 mol of Ru^{VI} (see the Experimental Section). Thus, the reaction of *trans*-[Ru^{VI}(tmc)(O)₂]²⁺ with H₂Q in CH₃CN can be represented by eqs 4 and 5.



The kinetics were monitored at 246 nm, and the data were fitted to a biexponential function.²⁰ The pseudo-first-order rate constants (k_{obs} and k'_{obs}) depend linearly on [H₂Q] but are independent of [Ru^{VI}]. The second-order rate constants (k_{ACN} and k'_{ACN}) for both steps are collected in Table 1. The effects of temperature were investigated from 288.0 to 318.0 K in CH₃CN. ΔH^\ddagger and ΔS^\ddagger are 12.3 ± 0.3 kcal mol⁻¹ and $-(9 \pm 1)$ cal mol⁻¹ K⁻¹, respectively, for the k_{ACN} path (first step) and 12.4 ± 0.3 kcal mol⁻¹ and $-(15 \pm 2)$ cal mol⁻¹ K⁻¹, respectively, for the k'_{ACN} path (second step).

Table 2. Thermodynamic Data for Hydroquinones

H ₂ Q-X	BDE/kcal mol ⁻¹ ^a	pK _a	E°(Q-X/H ₂ Q-X)/V
2,5-di-'Bu	79.0		0.562 ^b
'Bu	79.6	10.22 ^c	0.628 ^c
2,3-di-Me	79.9		
Me	80.3	10.05 ^c	0.644 ^c
OMe	80.9	9.91 ^c	0.594 ^c
H	82.3	9.85 ^c	0.699 ^c
Cl	83.3	8.90 ^c	0.712 ^c
2,3-di-CN	88.6	5.5 ^d	0.910 ^c

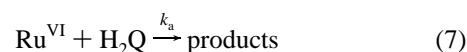
^a BDE = O-H bond dissociation energy, calculated according to ref 24. ^b From ref 25. ^c From ref 7. ^d From ref 5.

The kinetics of the oxidations of H₂Q-X were also studied in CH₃CN, and the rate constants are shown in Table 1. A few experiments were done by using *trans*-[Ru^{IV}(tmc)(O)(CH₃CN)]²⁺ as the oxidant, and the rate constants obtained were the same as k'_{ACN} .

Discussion

Reactions in H₂O. In the presence of excess H₂Q, *trans*-[Ru^{VI}(tmc)(O)₂]²⁺ was rapidly reduced to *trans*-[Ru^{IV}(tmc)(O)(OH)₂]²⁺ in H₂O. No intermediate Ru^V species was observed, as in the reaction of *trans*-[Ru^{VI}(tmc)(O)₂]²⁺ with a number of other reducing agents.¹⁵⁻¹⁷ In aqueous acidic solutions, *trans*-[Ru^V(tmc)(O)(OH)]²⁺ is a stronger oxidant than *trans*-[Ru^{VI}(tmc)(O)₂]²⁺; once formed it will either be reduced more rapidly than Ru^{VI} or undergo rapid disproportionation.¹⁸ Further reduction of Ru^{IV} to Ru^{III} or Ru^{II} does not occur. Thermodynamically, the [Ru^{VI}(tmc)(O)₂]²⁺/[Ru^{IV}(tmc)(O)(OH)₂]²⁺ couple is capable of oxidizing H₂Q-X to Q-X (Scheme 2 and Table 2). However, although the [Ru^{IV}(tmc)(O)(OH)₂]²⁺/[Ru^{III}(tmc)(OH)₂]³⁺ couple should also be able to oxidize some of the substrates such as H₂Q-OMe and H₂Q-di-'Bu, the reactions are probably too slow to be observed at room temperature.

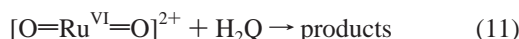
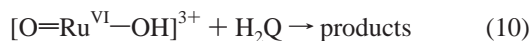
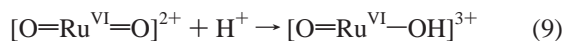
In aqueous solutions, the observed acid dependence of $k_{\text{H}_2\text{O}}$ is consistent with parallel pathways involving the oxidation of H₂Q and HQ⁻ (eqs 6-8).



Oxidation of Hydroquinones

k_a and k_b correspond to the rate constants for the reduction of Ru^{VI} by H_2Q and HQ^- , respectively. According to this scheme, the rate law is given by eq 3.

The observed acid dependence may also be accounted for by a pathway that involves protonated Ru^{VI} species (eqs 9–11).



This pathway is rejected because there is no evidence for protonation of Ru^{VI} even in 6 M acid. Moreover, the oxidation of substrates with no acidic protons, such as $[\text{Ru}(\text{NH}_3)_4(\text{bpy})]^{2+}$ ($\text{bpy} = 2,2'$ -bipyridine), is independent of pH from 1 to 5.¹⁸

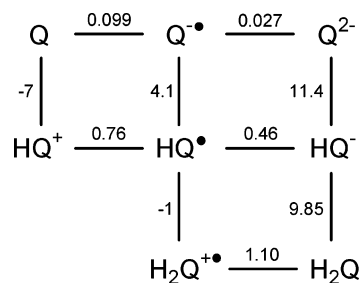
In aqueous solutions at pH = 1.79, where the pathway involving the oxidation of HQ^- is insignificant, a large kinetic isotope effect for the oxidation of H_2Q in D_2O [$k(\text{H}_2\text{O})/k(\text{D}_2\text{O}) = 4.9$] was observed. However, no kinetic isotope effect was found for the oxidation of $\text{H}_2\text{Q}-d_6$ in H_2O [$k[\text{C}_6\text{H}_4(\text{OH})_2]/k[\text{C}_6\text{D}_4(\text{OH})_2] = 1.0$]. These results suggest that the rate-determining step for the oxidation of the H_2Q molecule involves O–H bond cleavage. On the other hand, at pH = 4.60, in which the oxidation of the HQ^- anion is the predominant pathway, a negligible kinetic isotope effect of 1.2 ± 0.2 was found for the oxidation of H_2Q in D_2O .

Reactions in CH_3CN . In contrast to the reaction in H_2O , two steps are observed in CH_3CN for the reduction of $\text{trans}-[\text{Ru}^{\text{VI}}(\text{tmc})(\text{O})_2]^{2+}$ by $\text{H}_2\text{Q}-\text{X}$. The first step is the reduction of $\text{trans}-[\text{Ru}^{\text{VI}}(\text{tmc})(\text{O})_2]^{2+}$ to $\text{trans}-[\text{Ru}^{\text{IV}}(\text{tmc})(\text{O})(\text{CH}_3\text{CN})]^{2+}$, while the second step corresponds to the reduction of $\text{trans}-[\text{Ru}^{\text{IV}}(\text{tmc})(\text{O})(\text{CH}_3\text{CN})]^{2+}$ to $\text{trans}-[\text{Ru}^{\text{II}}(\text{tmc})(\text{CH}_3\text{CN})_2]^{2+}$, as shown in eqs 4 and 5, respectively. For the first step, the aquo species, $\text{trans}-[\text{Ru}^{\text{IV}}(\text{tmc})(\text{O})(\text{OH}_2)]^{2+}$, is probably formed initially (eq 1), followed by rapid solvolysis to give the CH_3CN complex. Similarly, for the second step, the species $\text{trans}-[\text{Ru}^{\text{II}}(\text{tmc})(\text{OH}_2)(\text{CH}_3\text{CN})]^{2+}$ is probably formed initially.

CH_3CN is a π -acid ligand that has a high affinity for Ru^{II} . For example, E° for $[\text{Ru}(\text{NH}_3)_5(\text{OH}_2)]^{3+/2+}$ and $[\text{Ru}(\text{NH}_3)_5(\text{CH}_3\text{CN})]^{3+/2+}$ are 0.067 and 0.426 V (vs NHE), respectively.²⁶ If a similar shift of 0.36 V occurs for $\text{Ru}^{\text{II}}(\text{tmc})$, then E° for the $[\text{Ru}^{\text{IV}}(\text{tmc})(\text{O})(\text{CH}_3\text{CN})]^{2+}/[\text{Ru}^{\text{II}}(\text{tmc})(\text{OH}_2)(\text{CH}_3\text{CN})]^{2+}$ couple would be around 0.95 V. The higher redox potential in CH_3CN explains why Ru^{IV} is able to oxidize $\text{H}_2\text{Q}-\text{X}$ in CH_3CN but not in H_2O .

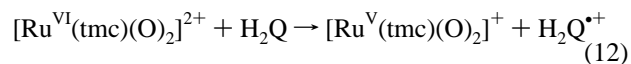
Mechanisms. In the reduction of Ru^{VI} to Ru^{IV} by H_2Q in H_2O (k_a path) or in CH_3CN , there are four possible

Scheme 3

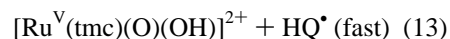
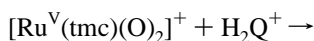


mechanisms, similar to those described by Meyer for the reduction of $[(\text{bpy})_2(\text{py})\text{Ru}^{\text{IV}}=\text{O}]^{2+}$ by H_2Q :¹¹

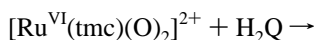
(1) initial electron transfer followed by rapid proton transfer



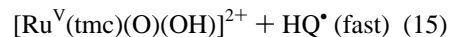
$$(\Delta G^\circ = 12.5 \text{ kcal mol}^{-1})$$



(2) initial proton transfer followed by electron transfer

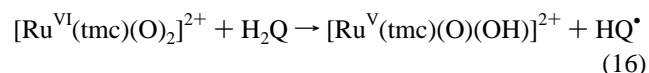


$$(\Delta G^\circ = > 14.8 \text{ kcal mol}^{-1})$$



(3) H-atom transfer (HAT; concerted one-electron,

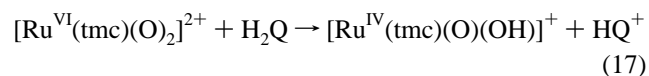
one-proton transfer)²⁷



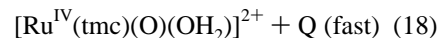
$$(\Delta G^\circ = 8.6 \text{ kcal mol}^{-1})$$

(4) hydride transfer

(concerted two-electron, one-proton transfer)



$$(\Delta G^\circ = 6.2 \text{ kcal mol}^{-1} \text{ in } \text{H}_2\text{O})$$



ΔG° for each pathway was calculated based on the thermodynamic data for Ru^{VI} in Scheme 2 and for H_2Q in Scheme 3.^{11,28}

(24) Wright, J. S.; Johnson, E. R.; DiLabio, G. A. *J. Am. Chem. Soc.* **2001**, *123*, 1173–1183.

(25) Evans, D. H. In *Encyclopedia of Electrochemistry of the Elements. Organic Section*; Bard, A. J., Ed.; Marcel Dekker: New York, 1976; Vol. XII.

(26) Matsubara, T.; Ford, P. C. *Inorg. Chem.* **1976**, *15*, 1107–1110.

(27) HAT may be regarded as a subset of PCET. For discussions of HAT and PCET, see: (a) Mayer, J. M. *Annu. Rev. Phys. Chem.* **2004**, *55*, 363–390. (b) Mayer, J. M.; Rhile, I. J. *Biochim. Biophys. Acta* **2004**, *1655*, 51–58.

(28) Laviron, E. J. *Electroanal. Chem.* **1984**, *169*, 29–46.

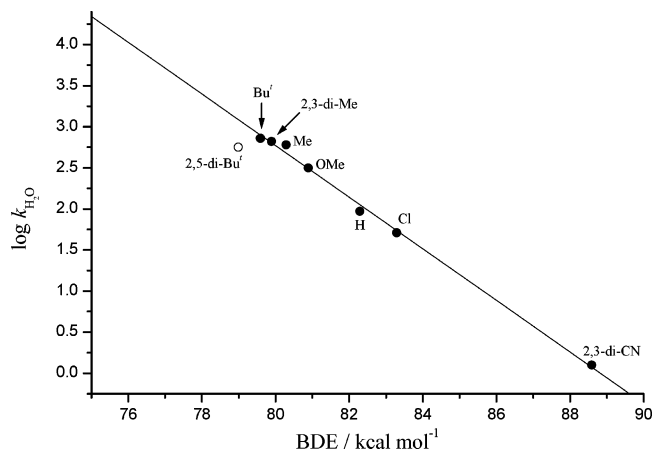


Figure 4. Plot of $\log k_{\text{H}_2\text{O}}$ vs O–H BDE for the oxidation of $\text{H}_2\text{Q-X}$ by $\text{trans-}[\text{Ru}^{\text{VI}}(\text{tmc})(\text{O})_2]^{2+}$ in aqueous solutions at 298.0 K, pH = 1.77 and $I = 0.1$ M (slope = -0.31 ± 0.01 ; y intercept = 27.86 ± 0.67 ; $r = 0.998$).

For the initial electron transfer, ΔG° is only lower than ΔG^\ddagger ($14.7 \text{ kcal mol}^{-1}$) by around 2 kcal mol^{-1} , suggesting that this pathway is rather unlikely. An estimation of the theoretical rate constant for outer-sphere electron transfer (k_{12}) can be made using the Marcus cross relation,²⁹ eqs 19 and 20 (neglecting work terms). K_{12} , the equilibrium constant

$$k_{12} = (k_{11}k_{22}K_{12}f_{12})^{1/2} \quad (19)$$

$$\log f_{12} = \frac{(\log K_{12})^2}{4 \log(k_{11}k_{22}/10^{22})} \quad (20)$$

for the reaction, is calculated from the reduction potentials for the $[\text{Ru}^{\text{VI}}(\text{tmc})(\text{O})_2]^{2+}/[\text{Ru}^{\text{V}}(\text{tmc})(\text{O})_2]^+$ and $\text{H}_2\text{Q}^+/\text{H}_2\text{Q}$ couples to be 2.5×10^4 . A value of $1 \times 10^5 \text{ M}^{-1} \text{ s}^{-1}$ is used for k_{11} , the self-exchange rate for $[\text{Ru}^{\text{VI}}(\text{tmc})(\text{O})_2]^{2+}/[\text{Ru}^{\text{V}}(\text{tmc})(\text{O})_2]^+$,¹⁸ k_{22} , the self-exchange rate for $\text{H}_2\text{Q}^+/\text{H}_2\text{Q}$, is taken as $2 \times 10^6 \text{ M}^{-1} \text{ s}^{-1}$.⁵ Using these data, k_{12} is calculated to be $1.2 \text{ M}^{-1} \text{ s}^{-1}$ at 298 K, which is almost 2 orders of magnitude slower than the experimental rate constant ($9.4 \times 10^1 \text{ M}^{-1} \text{ s}^{-1}$), again suggesting that this mechanism is unlikely.

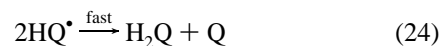
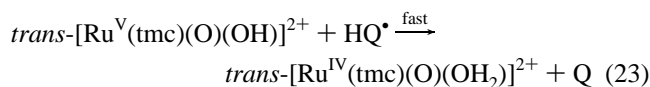
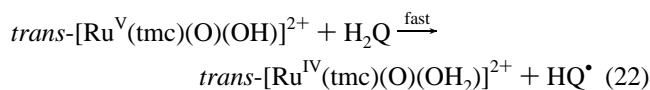
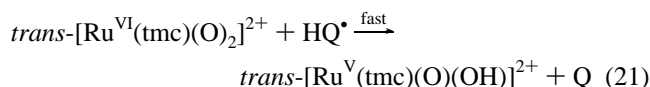
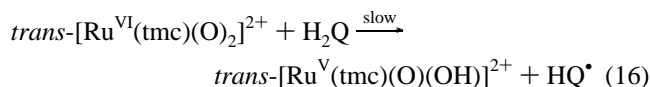
The initial proton-transfer mechanism can be ruled out because $\Delta G^\circ > \Delta G$. On the other hand, the HAT and hydride-transfer mechanisms have much lower ΔG° values and are more feasible mechanisms. The hydride-transfer mechanism is less likely than HAT for the following reasons. $\text{H}_2\text{Q-2,3-di-Me}$ is oxidized at about the same rate as $\text{H}_2\text{Q-Me}$ and is only 6 times faster than H_2Q . Similarly, $\text{H}_2\text{Q-Cl}$ is oxidized by less than 2 times slower than H_2Q . A hydride mechanism with a partially cationic hydroquinone transition state should be much more susceptible to substituent effects. For the same reason, a hydride-transfer mechanism should be rather sensitive to solvent effects; however, reactions in water are only slightly faster than those in CH_3CN . Further support of HAT over hydride transfer comes from a study of the relation between the rates and O–H bond dissociation energies (BDEs) of $\text{H}_2\text{Q-X}$.

(29) Marcus, R. A.; Eyring, H. *Annu. Rev. Phys. Chem.* **1964**, *15*, 155–196.

For the oxidation of HQ^- (k_b pathway), an estimation of the theoretical rate constant for outer-sphere electron transfer can also be made using the Marcus equations (eqs 19 and 20) and a self-exchange rate of 2×10^6 for the HQ^*/HQ^- couple.⁵ The calculated rate constant is $3.1 \times 10^6 \text{ M}^{-1} \text{ s}^{-1}$ at 298 K, which is not too different from the experimental value of $7.9 \times 10^7 \text{ M}^{-1} \text{ s}^{-1}$. The negligible deuterium isotope effects are also in agreement with an electron-transfer mechanism, although it is possible that there may be some hydrogen-bonding effects in the transition state.

The mechanism for the oxidation of H_2Q by $\text{trans-}[\text{Ru}^{\text{VI}}(\text{tmc})(\text{O})_2]^{2+}$ in aqueous acidic solutions (pH < 3) is summarized in Scheme 4.

Scheme 4



HQ^\bullet is known to disproportionate rapidly ($k = 1.1 \times 10^9 \text{ M}^{-1} \text{ s}^{-1}$).³⁰

Correlation between Rate Constants and O–H BDEs of Hydroquinones. Mayer and co-workers have shown that for PCET/HAT reactions the rates should correlate with the bond strengths of the substrates.³¹ We found that linear correlations were obtained for the oxidation of $\text{H}_2\text{Q-X}$ by Ru^{VI} in both H_2O and CH_3CN when $\log(\text{rate constant})$ at 298.0 K was plotted against the O–H BDEs of $\text{H}_2\text{Q-X}$ (Figures 4 and 5). In these plots, the O–H BDEs calculated according to the method of Wright and co-workers were used (Table 2)²⁴ because we could only find experimental data for a few substrates such as H_2Q and $\text{H}_2\text{Q-Me}$. Similar correlations have also been observed in the oxidation of hydrocarbons by CrO_2Cl_2 ,³² ${}^n\text{Bu}_4\text{NMnO}_4$,^{31c} and $\text{trans-}[\text{Ru}^{\text{VI}}(\text{N}_2\text{O}_2)(\text{O})_2]^{2+}$ ³³ and in the oxidation of phenols by $\text{trans-}[\text{Ru}^{\text{VI}}(\text{N}_2\text{O}_2)(\text{O})_2]^{2+}$.³⁴ Notably, $\text{H}_2\text{Q-2,5-di-}^t\text{Bu}$ reacts more slowly than expected from its BDE, by about 50%. The

(30) Adams, G. E.; Michael, B. D. *Trans. Faraday Soc.* **1967**, *63*, 1171–1180.

(31) (a) Bryant, J. R.; Mayer, J. M. *J. Am. Chem. Soc.* **2003**, *125*, 10351–10361. (b) Mayer, J. M. *Acc. Chem. Res.* **1998**, *31*, 441–450. (c) Gardner, K. A.; Kuehnert, L. L.; Mayer, J. M. *Inorg. Chem.* **1997**, *36*, 2069–2078.

(32) Cook, G. K.; Mayer, J. M. *J. Am. Chem. Soc.* **1995**, *117*, 7139–7156.

(33) Lam, W. W. Y.; Yiu, S. M.; Yiu, D. T. Y.; Lau, T. C.; Yip, W. P.; Che, C. M. *Inorg. Chem.* **2003**, *42*, 8011–8018.

(34) Yiu, D. T. Y.; Lee, M. F. W.; Lam, W. W. Y.; Lau, T. C. *Inorg. Chem.* **2003**, *42*, 1225–1232.

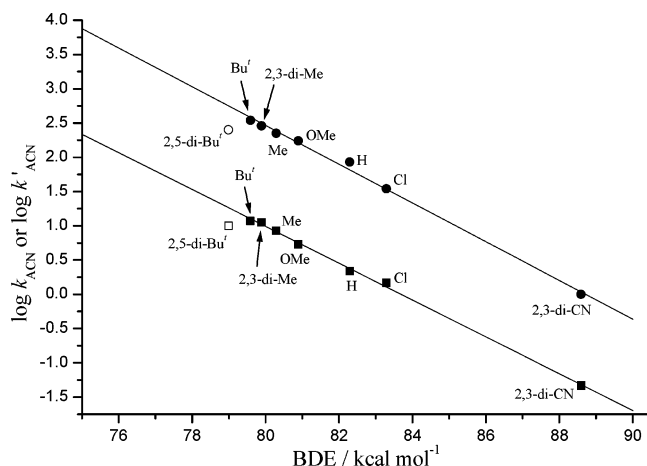


Figure 5. Plot of $\log k_{\text{ACN}}$ (circles) and $\log k'_{\text{ACN}}$ (squares) vs O–H BDE for the oxidation of $\text{H}_2\text{Q-X}$ by $\text{trans-}[\text{Ru}^{\text{VI}}(\text{tmc})(\text{O})_2]^{2+}$ and $\text{trans-}[\text{Ru}^{\text{IV}}(\text{tmc})(\text{O})(\text{CH}_3\text{CN})]^{2+}$, respectively, at 298.0 K in CH_3CN . (For the k_{ACN} path, slope = -0.28 ± 0.01 , y intercept = 25.11 ± 0.65 , and $r = 0.998$. For the k'_{ACN} path, slope = -0.27 ± 0.01 , y intercept = 22.49 ± 0.42 , and $r = 0.999$.)

presence of two bulky groups in the 2 and 5 positions should reduce the chance of H-atom abstraction by the bulky $\text{trans-}[\text{Ru}^{\text{VI}}(\text{tmc})(\text{O})_2]^{2+}$ complex by about 50%. Such steric effects are expected for a HAT mechanism but not for simple electron transfer.

Application of the Marcus Cross Relation. Mayer and co-workers have recently shown that the Marcus cross relation (eq 19; neglecting work terms) holds fairly well for a range of PCET/HAT reactions.^{27a,35}

For reactions where the frequency factors, f_{12} , are close to 1, eq 19 is simplified to eq 25. k_{12} is the rate constant for

$$k_{12} = (k_{11}k_{22}K_{12})^{1/2} \quad (25)$$

the reaction between reactants **1** and **2**. k_{11} and k_{22} are the H-atom self-exchange rates of the reactants. The equilibrium constant, K_{12} , for the oxidation of $\text{H}_2\text{Q-X}$ by Ru^{VI} is calculated from $\Delta G^\circ = -RT \ln K_{12}$, using $\Delta G^\circ \approx \Delta H^\circ = \text{O-H BDE of H}_2\text{Q-X} - \text{BDE of } [\text{O}=\text{Ru}^{\text{V}}(\text{tmc})\text{O-H}]^{2+}$. It is assumed that ΔS° values for these reactions are relatively small. The BDE of $[\text{O}=\text{Ru}^{\text{V}}(\text{tmc})\text{O-H}]^{2+}$ is calculated to be $73.7 \text{ kcal mol}^{-1}$ in aqueous solutions and $76.3 \text{ kcal mol}^{-1}$ in CH_3CN according to the equation $D[\text{O}=\text{Ru}^{\text{V}}(\text{tmc})\text{O-H}] = 23.06E^\circ + 1.37\text{p}K_a + C$.^{31b,36–39} E° for $[\text{Ru}^{\text{VI}}(\text{tmc})(\text{O})_2]^{2+}/[\text{Ru}^{\text{V}}(\text{tmc})(\text{O})_2]^{2+} = 0.56 \text{ V}$ (vs NHE),¹⁸ $\text{p}K_a$ of $[\text{O}=\text{Ru}^{\text{V}}(\text{tmc})\text{O-H}]^{2+} = 2.8$,¹⁸ $C = 57$ and $59.5 \text{ kcal mol}^{-1}$ respectively in aqueous solutions and in CH_3CN .^{36,40}

- (35) (a) Roth, J. P.; Yoder, J. C.; Won, T.-J.; Mayer, J. M. *Science* **2001**, *294*, 2524–2526. (b) Roth, J. P.; Mayer, J. M. *Inorg. Chem.* **1999**, *38*, 2760–2761. (c) Roth, J. P.; Lovell, S.; Mayer, J. M. *J. Am. Chem. Soc.* **2000**, *122*, 5486–5498.
- (36) Mayer, J. M. In *Biomimetic Oxidations Catalyzed by Transition Metal Complexes*; Meunier, B., Ed.; Imperial College Press: London, 2000; pp 1–43.
- (37) Wayner, D. D. M.; Luszyk, E.; Pagé, D.; Ingold, K. U.; Mulder, P.; Laarhoven, L. J. J.; Aldrich, H. S. *J. Am. Chem. Soc.* **1995**, *117*, 8737–8744.
- (38) Parker, V. D. *J. Am. Chem. Soc.* **1992**, *114*, 7458–7462.
- (39) Parker, V. D.; Tilset, M. *J. Am. Chem. Soc.* **1989**, *111*, 6711–6717.
- (40) Skagestad, V.; Tilset, M. *J. Am. Chem. Soc.* **1993**, *115*, 5077–5083.

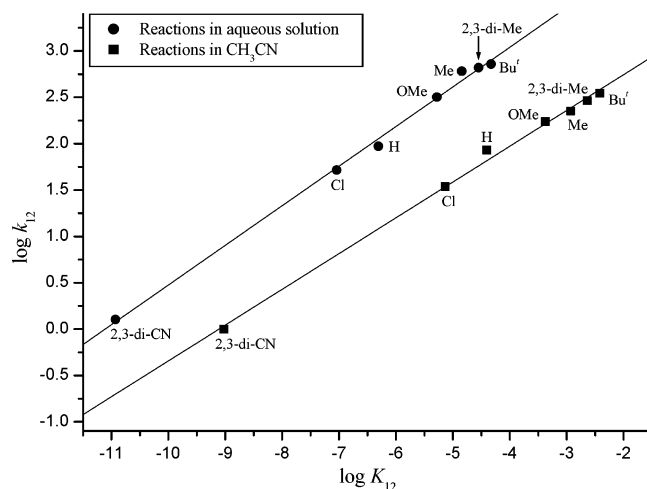


Figure 6. Plot of $\log k_{12}$ vs $\log K_{12}$ for the oxidation of $\text{H}_2\text{Q-X}$ by $\text{trans-}[\text{Ru}^{\text{VI}}(\text{tmc})(\text{O})_2]^{2+}$ at 298.0 K in aqueous solutions (circles) and in CH_3CN (squares). (In aqueous solutions, slope = 0.43 ± 0.01 , y intercept = 4.03 ± 0.06 , and $r = 0.998$. In CH_3CN , slope = 0.39 ± 0.01 , y intercept = 3.52 ± 0.05 , and $r = 0.998$.)

Figure 6 shows plots of $\log k_{12}$ vs $\log K_{12}$ for the reduction of Ru^{VI} to Ru^{IV} by $\text{H}_2\text{Q-X}$ in H_2O and in CH_3CN . Good linear correlations are obtained; the slopes of 0.43 ± 0.01 and 0.39 ± 0.01 for H_2O and CH_3CN , respectively, are in reasonable agreement with the theoretical slope of 0.5 predicted by eq 25. Such linear plots imply that the H-atom self-exchange rates of $\text{H}_2\text{Q-X}$ are similar. From the y intercepts, which are equal to $(1/2) \log(k_{11}k_{22})$ according to eq 25, $k_{11}k_{22} = 1.1 \times 10^8$ and $1.1 \times 10^7 \text{ M}^{-2} \text{ s}^{-2}$ for H_2O and CH_3CN , respectively. If we take $3 \times 10^4 \text{ M}^{-1} \text{ s}^{-1}$ as the H-atom self-exchange rate of $\text{H}_2\text{Q-X}$ in CH_3CN ,^{35a} then the $[\text{Ru}^{\text{VI}}(\text{tmc})(\text{O})_2]^{2+}/[\text{Ru}^{\text{V}}(\text{tmc})(\text{O})(\text{OH})]^{2+}$ self-exchange rate in CH_3CN is estimated to be $4 \times 10^2 \text{ M}^{-1} \text{ s}^{-1}$. The higher $k_{11}k_{22}$ value in water could be due to a higher H-atom self-exchange rate for either one or both of the reactants in water. Similar treatment of the data for the reduction of $\text{trans-}[\text{Ru}^{\text{IV}}(\text{tmc})(\text{O})(\text{CH}_3\text{CN})]^{2+}$ to $\text{trans-}[\text{Ru}^{\text{II}}(\text{tmc})(\text{CH}_3\text{CN})_2]^{2+}$ was not carried out because the BDE of $[(\text{CH}_3\text{CN})\text{Ru}^{\text{III}}(\text{tmc})\text{O-H}]^{2+}$ is not known.

Conclusions

The oxidation of a series of $\text{H}_2\text{Q-X}$ compounds by $\text{trans-}[\text{Ru}^{\text{VI}}(\text{tmc})(\text{O})_2]^{2+}$ in aqueous solutions and in CH_3CN , and by $\text{trans-}[\text{Ru}^{\text{IV}}(\text{tmc})(\text{O})(\text{CH}_3\text{CN})]^{2+}$ in CH_3CN , occurs by initial, rate-limiting H-atom abstraction. This is supported by a large solvent kinetic isotope effect [$k(\text{H}_2\text{O})/k(\text{D}_2\text{O}) = 4.9$] and linear correlations between $\log(\text{rate constants})$ and O–H BDE of $\text{H}_2\text{Q-X}$. The Marcus cross relation appears to hold reasonably well for these HAT reactions.

Acknowledgment. The work described in this paper was supported by a grant from the Research Grants Council of Hong Kong (CityU 1105/02P).

Supporting Information Available: Table of second-order rate constants, plots of k_{obs} vs $[\text{H}_2\text{Q-X}]$ for the oxidation of $\text{H}_2\text{Q-X}$ by $\text{trans-}[\text{Ru}^{\text{IV}}(\text{tmc})(\text{O})_2]^{2+}$ in aqueous solutions and CH_3CN and of k'_{obs} vs $[\text{H}_2\text{Q-X}]$ for the oxidation of $\text{H}_2\text{Q-X}$ by $\text{trans-}[\text{Ru}^{\text{IV}}(\text{tmc})(\text{O})_2]^{2+}$ in CH_3CN , and Eyring plots for the oxidation of H_2Q by $\text{trans-}[\text{Ru}^{\text{IV}}(\text{tmc})(\text{O})_2]^{2+}$ in aqueous solutions and CH_3CN .

IC0513821